Korean J. Chem. Eng., 38(2), 316-325 (2021)
DOI: 10.1007/s11814-020-0698-8

pISSN: 0256-1115
eISSN: 1975-7220

Removal efficiency optimization of Pb^{2+} in a nanofiltration process by MLP-ANN and RSM

Mohammad Reza Sarmasti Emami†, Mahmoud Kiannejad Amiri, and Seyed Peiman Ghorbanzade Zaferani

Department of Chemical Engineering, University of Science and Technology of Mazandaran, Behshahr, Iran
(*Received 22 July 2020 • Revised 4 October 2020 • Accepted 17 October 2020*)

Abstract−Using computational intelligence for prediction, modeling, and optimization of chemical process behavior could save costs and time. This study's main goal was to predict and optimize removal efficiency and permeate flux behavior of Pb^{2+} aqueous solution in a nanofiltration process through using response surface methodology (RSM) and multilayer perceptron (MLP) neural network. A regression coefficient R^2=0.99 was obtained for both removal efficiency and permeate flux in the RSM model. Also, the F-value for the removal efficiency and permeate flux was 394.79 and 1888.85, respectively. Different MLP structures for predicting removal efficiency and permeate flux behavior of lead ion in aqueous solutions were investigated. The best structure was obtained for two hidden layers with nine (tansig transfer function) and three (logsig transfer function) neurons. The values of R=0.9993, R^2=0.9986, MSE=0.402 and MAE=0.409 for the best structure were obtained. Finally, the the removal efficiency was optimized through RSM based on the experimental data. It was concluded that optimum mode selected for membrane composition of PSF=10.04%, NMP=88.98%, and PAN-CMC-41=0.98% (wt%) 53.17 ppm as lead ion concentration in solution and 30.31 min for filtration time achieved the maximum value of removal efficiency equal to 90.68%.

Keywords: Membrane, Modeling, Prediction, RSM, MLP, Lead Ion, Filtration

INTRODUCTION

Severe global environmental issues and lack of energy are primary concerns of governments recently. In this regard, environmental management and energy management are the fundamental strategies that used to achieve environmental and economic targets. One of the main steps for environmental management is finding solutions to environmental challenges. The pollution challenge is one of the serious global environmental issues that has affected many a person's life worldwide [1-3]. The main reason for the pollution challenge in the last 30 years is industrialization, due to the fast-growing global population. One of the primary resources of such pollution is the heavy metal issue. Researches have shown that these metals, like Cadmium, Lead, and Mercuryare toxic [4,5]. Entering industrial wastewater, the primary food resource of humans, animals, and plants gets polluted in the soils and rivers [6].

Many methods have been tested for water treatment operations in the world. One of the best methods for solving the heavy metals issue is the membrane-based separation system that is very useful for industrial applications [7]. The mentioned systems have advantages like flexibility, a choose able operating state, excellent efficiency, and low energy. Researchers have recently applied nanotechnology in membrane systems such as nanofiltration due to high water permeability and low operating pressure compared to other filtration methods [8,9].

In this regard, many studies have investigated the effect of nanoparticles on the different polymer-based membranes. One of the polymers selected for this technique is Polysulfone (PSF) due to economic aspects and appropriate physical properties [10-16]. Alawady et al. [17] investigated the effects of adding carbon nanotubes (CNTs) and CNTS-COOH to Chitosan/polysulfone membranes in the rejection of different metal ions. They reported that adding carboxylic groups on CNTs has improved the performance of the membrane. Modi and Bellare [18] fabricated a hybrid polysulfone-iron oxide/graphene oxide composite hollow fiber membrane to remove phenolic compounds from an aqueous medium moving in a stream. Zhu et al. [19] evaluated the effects of incorporating different content of TiO_2 to graphene oxide (GO)/PSF membrane. They concluded that adding TiO_2 to the membrane has improved water permeability and the novel membrane's performance. Kumar et al. [20] used a PSF composite with another component as a UF membrane to remove heavy metals. They reported the membrane with a composition of PSF/N-succinyl Chitosan (80 : 20) showed excellent performance and high rejection of heavy metals.

The use of computational intelligence and numerical math methods for prediction, modeling, and optimization of chemical process behavior and evaluating the parameters that affected the process has been growing in recent years. Also, it could be saving cost and time by using these methods [21-30]. For this purpose, Table 1 shows a review of different modeling and optimization methods in various membrane systems.

Tiwari et al. [39] used response surface methodology (RSM) to find the optimum state of copper recovery with a membrane separation system. They reported three factors (operating pressure, initial concentration, and inlet flow rate) are mainly affected by the separation process. They used the second-order polynomial equation for the study. Finally, they concluded that the RSM is an excellent method to predict and optimize of the parameters of membrane

†To whom correspondence should be addressed.
E-mail: m_r_emami@mazust.ac.ir

Table 1. Review of the application of different modeling methods in various membrane systems

Reference	Year	Membrane	Modeling and optimization method
[31]	2020	Fe/PAN, Goe/PAN, Mf/PAN	Response Surface Methodology
[32]	2020	MOF-2(Cd)/PI MMMs	Response Surface Methodology
[33]	2020	MBR	Artificial Neural Network
[34]	2019	MWCNTs/PPy	Artificial Neural Network
[35]	2019	GO-MWCNT/PVDF	Response Surface Methodology
[36]	2018	AO-MBR	Artificial Neural Network
[37]	2017	ELM	Response Surface Methodology
[38]	2016	Ceramic membrane	Artificial Neural Network

systems. Alver and Kazan [40] evaluated the effects of different parameters on a reverse osmosis membrane system's performance by using an artificial neural network (ANN) evaluating the effects of different parameters on a reverse osmosis membrane system by using an artificial neural network (ANN). They investigated different structures with Levenberg-Marquardt as a learning method. They found that the artificial neural network shows excellent performance for modeling of a reverse osmosis membrane system. In another study, Choudhury et al. [41] fabricated a UF membrane with content of CuO nanoparticles for removing heavy metals and optimized the experimental condition through RSM. They reported that using RSM optimization is very useful in finding the best conditions for fabricating the membrane. For comparing the performance of the methods, Jun et al. [42] used RSM and artificial neural networks coupled with PSO to model and optimize the crucial parameters of functionalized bipolar/PVA membrane for removing methylene blue dye from aqueous solution. They concluded that ANN-particle swarm optimization (PSO) had shown excellent performance for predicting the removal contamination process parameters by JP functionalized BP/PVA membrane.

The present study aimed to model, predict, and optimize removal efficiency and permeate flux behavior of lead ion in aqueous solution in a nanofiltration process. Polysulfone (PSF) blended with polyaniline (PAN)/nanoparticles mixed matrix membrane was used in this process. The modeling and optimization are based on the study's experimental results by Toosi et al. [43]. These experimental results include filtration time, the concentration of lead ion solution, the amount of PSF, NMP, and PAN-CMC-41. Removal efficiency and flux behavior of lead ion in solutions were modeled and predicted using RSM and multilayer perceptron artificial neural network. After that, both methods were compared, till which method performed better.

Finally, the removal efficiency of Pb^{2+} was optimized through RSM in a different mode. RSM optimization was done for obtaining the optimum composition of the mixed matrix membrane in the nanofiltration process to gain high removal efficiency. The optimization of the removal efficiency of Pb^{2+} can save costs and time of different experimental work.

MODELING DESCRIPTION

1. Response Surface Methodology

One of the methods used to find a relationship between useful parameters and outputs of a process is response surface methodology. Also, the significance of the useful parameters has been investigated by RSM. The experiment's costs will be decreased due to the optimization of the useful parameters [44]. A matrix that related parameters to the response was used for designing the experiment through RSM. The matrix is composed of experimental data, error terms, and interaction coefficients. The main task of RSM is to build a function that relates experimental data to the outputs of the model that had been predicted by the function [45]. The outputs of the RSM model have been called the response. Eq. (1) is shown in the response definition:

$$y=X\beta+\varepsilon_y \tag{1}$$

Hence, y is the response, X is an input vector of the model, β is an unknown coefficient vector, and ε_y shows the error vector. We used a polynomial equation for fitting experimental data versus response; for a second-order polynomial equation, the equation can be illustrated as below [46]:

$$y=\beta_0+\sum\beta_i X_i+\sum\beta_{ij}X_iX_j+\sum\beta_{ii}X_i^2+\varepsilon_y \tag{2}$$

1-1. Analysis of Variance

Analysis of variance (ANOVA) was applied for verifying the design model based on the experimental results. Two parameters that showed the importance of the model are F-value and p-value. High F-value and Probe>F less than 0.05 were assigned the primary criterion for significant models. Also, the coefficient of determination (R^2) was used for determining the explanation manner of model data based on experimental data [47]. R^2 was defined as the ratio of sum square of the model to sum square of y, as below:

$$R^2=\frac{SS_{mod}}{SS_{tot}}=1-\frac{SS_{res}}{SS_{tot}} \tag{3}$$

Hence, SS_{mod} was obtained the difference of the SS_{tot}, and sum square of the residual model. The closer it is to the unit, the higher the accuracy of the model. In some studies, R^2_{adj} is also evaluated as follows:

$$R^2_{adj}=1-\frac{SS_E/n-p}{SS_T/n-1}=1-\frac{n-1}{n-p}(1-R^2) \tag{4}$$

R^2_{adj} is reduced by adding too much of the parameter. This is the best way to add unnecessary variables in the R^2 unmodified model [48].

2. Multilayer Perceptron Artificial Neural Network

One smart method to predict and model the process is an arti-

ficial neural network (ANN). ANN is based on human brain performance; it means that ANN contains neurons and weights that obtain modeling and predicting the parameters. Also, the neurons communicate together through weights. Supervised, unsupervised, and hybrid are the three main learning paradigms for ANN training [49].

One of the most powerful methods for predicting ANN categories algorithms is the multilayer perceptron (MLP). The perceptron is a linear classifier. The main sections of the MLP-ANN structure are the input layer, the output layer, and the hidden layers (all the layers between the input and output layers). The hidden layer's task extracts the information from the initial data for processing through the neurons (that assigned biases for any of them). After that, an input is ready for transfer functions. By repetition, a sufficient number of perceptrons converge to the correct behavior [50].

We evaluated important network parameters of the MLP-NN for analyzing the performance of different structures of MLP-ANN. One of the factors is the mean squared error (MSE) that shows the relation average square error between outputs and inputs [51]. MSE was calculated as below:

$$MSE = \frac{1}{N}\sum_{i=0}^{N} e_i^2 \quad (5)$$

Other parameters are used for evaluating the precision of the training algorithm of various network structures called R^2. It can be defined as the following equation:

$$R^2 = \frac{\Sigma_{i=1}^{N}(A_i - \overline{A})^2 - \Sigma_{i=1}^{N}(P_i - \overline{p})^2}{\Sigma_{i=1}^{N}(A_i - \overline{A})^2} \quad (6)$$

where P_i is the value from the model, and A_i is the actual value. Another performance parameter used for this purpose is the root mean square error (RMSE) that can be calculated as follows:

$$RMSE = \sqrt{\frac{\Sigma_{i=0}^{N} e_i^2}{N}} \quad (7)$$

Hence, N is the number of data [52].

RESULTS AND DISCUSSION

1. Modeling with RSM

In this section, the modeled equations for predicting removal

Table 2. Analysis of variance (ANOVA) for removal efficiency of Pb^{2+}

Source	Sum of squares	df	Mean square	F-value	p-Value Prob>F
Model	13,901.48	19.00	731.66	394.79	0.00 significant
A-PSF	20.63	1.00	20.63	11.13	0.00
C-PAN-CMC-41	0.00	0.00			
D-Concentration	2,721.87	1.00	2,721.87	1,468.68	0.00
T-Time	209.11	1.00	209.11	112.83	0.00
AC	5.25	1.00	5.25	2.83	0.10
AD	2.04	1.00	2.04	1.10	0.30
AT	4.77	1.00	4.77	2.57	0.11
CD	0.00	0.00			
DT	18.86	1.00	18.86	10.18	0.00
A^2	0.00	0.00			
D^2	234.26	1.00	234.26	126.41	0.00
t^2	2.67	1.00	2.67	1.44	0.24
ACD	8.44	1.00	8.44	4.55	0.04
ADT	37.84	1.00	37.84	20.42	0.00
A^2D	0.00	0.00			
AD^2	4.79	1.00	4.79	2.59	0.11
D^2T	55.18	1.00	55.18	29.78	0.00
DT^2	167.68	1.00	167.68	90.48	0.00
T^3	90.69	1.00	90.69	48.94	0.00
A^2D^2	20.63	1.00	20.63	11.13	0.00
D^2T^2	15.03	1.00	15.03	8.11	0.01
DT^3	44.11	1.00	44.11	23.80	0.00
T^4	17.09	1.00	17.09	9.22	0.00
Residual	96.37	52.00	1.85		
Cor total	13,997.85	71.00			
Std. Dev.	1.36		R-Squared	0.99	
Mean	63.69		Adj R-Squared	0.99	
C.V. %	2.14		Pred R-Squared	0.98	

Table 3. Analysis of variance (ANOVA) for flux of Pb^{2+}

Source	Sum of squares	df	Mean square	F-value	p-Value Prob>F
Model	106,056.6	9	11,784.06	1,888.85	4.23E-72 significant
A-PSF	2,957.38	1	2,957.38	474.03	9.75E-31
B-NMP	0	0			
C-PAN-CMC-41	0	0			
D-Concentration	22,593.55	1	22,593.55	3,621.5	1.04E-56
E-Time	1,153.14	1	1,153.14	184.83	2.91E-20
AC	2,333.91	1	2,333.91	374.10	5.93E-28
AD	609.46	1	609.46	97.69	2.34E-14
CD	0	0			
DE	64.67	1	64.67	10.36	0.002044
B^2	0	0			
D^2	383.77	1	383.77	61.51	7.41E-11
ACD	238.71	1	238.71	38.26	5.39E-08
AD^2	69.38	1	69.38	11.12	0.001444
B^3	0	0			
Residual	386.80	62	6.23		
Cor total	106,443.4	71			
Std. Dev.	2.4		R-Squared	0.99	
Mean	91.13		Adj R-Squared	0.99	
C.V. %	2.74		Pred R-Squared	0.99	
PRESS	501.41		Adeq Precision	148.28	

efficiency and flux of lead ion in aqueous solution using PSF blended with PAN/nanoparticles mixed matrix membrane were investigated. Toosi et al. [43] reported three types, composition of the mixed matrix membrane as M1 (PSF=11.7%, NMP=88%, PAN-MCM41=0.3%), M2 (PSF=11.4%, NMP=88%, PAN-MCM41=0.6%), and M3 (PSF=10.8%, NMP=88%, PAN-MCM41=1.2%) based on weight percentage. Eqs. (8) and (9) describe the RSM modeling for determining the removal efficiency and flux of Pb^{2+} studied by Toosi et al. [43].

$$\begin{aligned}\text{Removal Efficiency}=&61.10-5.66A-15.43C-8.10t+5.61AB\\&-1.26AC-1.05At-2.66Ct+7.84C^2+2.20t^2\\&-5.03ABC+3.62ACt+3.34AC^2+2.84C^2t+5.00CT^2\\&-5.58t^3-13.63A^2C^2-2.59C^2t^2-4.77Ct^3+4.86t^4\end{aligned} \quad (8)$$

$$\begin{aligned}\text{Flux}=&117.58-46.01A-36.85B-6.11C+68.33t+21.74AB\\&-1.77BC+6.28Ct-26.76B^2-5.56C^2\end{aligned} \quad (9)$$

Hence t is the time of the filtration process. A and B denote PSF and PAN weight percentages in membrane composition, respectively, and C is the concentration of a lead ion in aqueous solution. The analysis of variance (ANOVA) of the removal efficiency and flux of Pb^{2+} correlations is presented in Tables 2 and 3, respectively.

The model's removal efficiency and flux of Pb^{2+} in aqueous solution have a regression coefficient R^2=0.99. The regression model's importance for the removal efficiency and flux model is evident from the large F-value (respectively, 394.79 and 1,888.85) and the small p-value.

Fig. 1 illustrates the adaptation graph based on the experimental results and residuals graphs of the proposed RSM models for removal efficiency and flux functions. As shown in Fig. 1(a) and Fig. 1(c), the proximity of the diagonal line points indicates that the empirical results are in great compromise with predicted outputs. However, a more accurate model for prediction of the flux of Pb^{2+} was obtained. Most of the residual values are very near to 0 for both models (Fig. 1(b) and Fig. 1(d)). So, it could have resulted that the suggested model could predicate the removal efficiency and flux of Pb^{2+} in aqueous solution by using the nanofiltration process well.

Fig. 2 shows the 3D graphs of (a) removal efficiency and (b) flux of Pb^{2+} in solution. An increasing trend in the value of removal efficiency has been observed when the filtration time and concentration of a lead ion in aqueous solution decrease. The highest amount of removal efficiency was obtained at the lowest filtration time and concentration of the lead ion. While a similar trend was obtained for the flux of lead ion, although, for the flux model, the dependent of flux to lead ion concentration was more observable compare to the removal efficiency model.

Contour diagrams of (a) removal efficiency and (b) flux of Pb^{2+} in solution are presented in Fig. 3. These graphs show that the filtration time and concentration of Pb^{2+} are directly related to the removal efficiency. Although, in a higher concentration of a lead ion in solution, the filtration time is more effective than the concentration in the removal of Pb^{2+}. For the flux model, the effect of concentration is more significant than the filtration time.

2. Modeling with MLP

Fig. 4 illustrates the top eight neural network structures designed to predict the removal efficiency and flux of lead ion.

The precision values of these structures for the designed neural

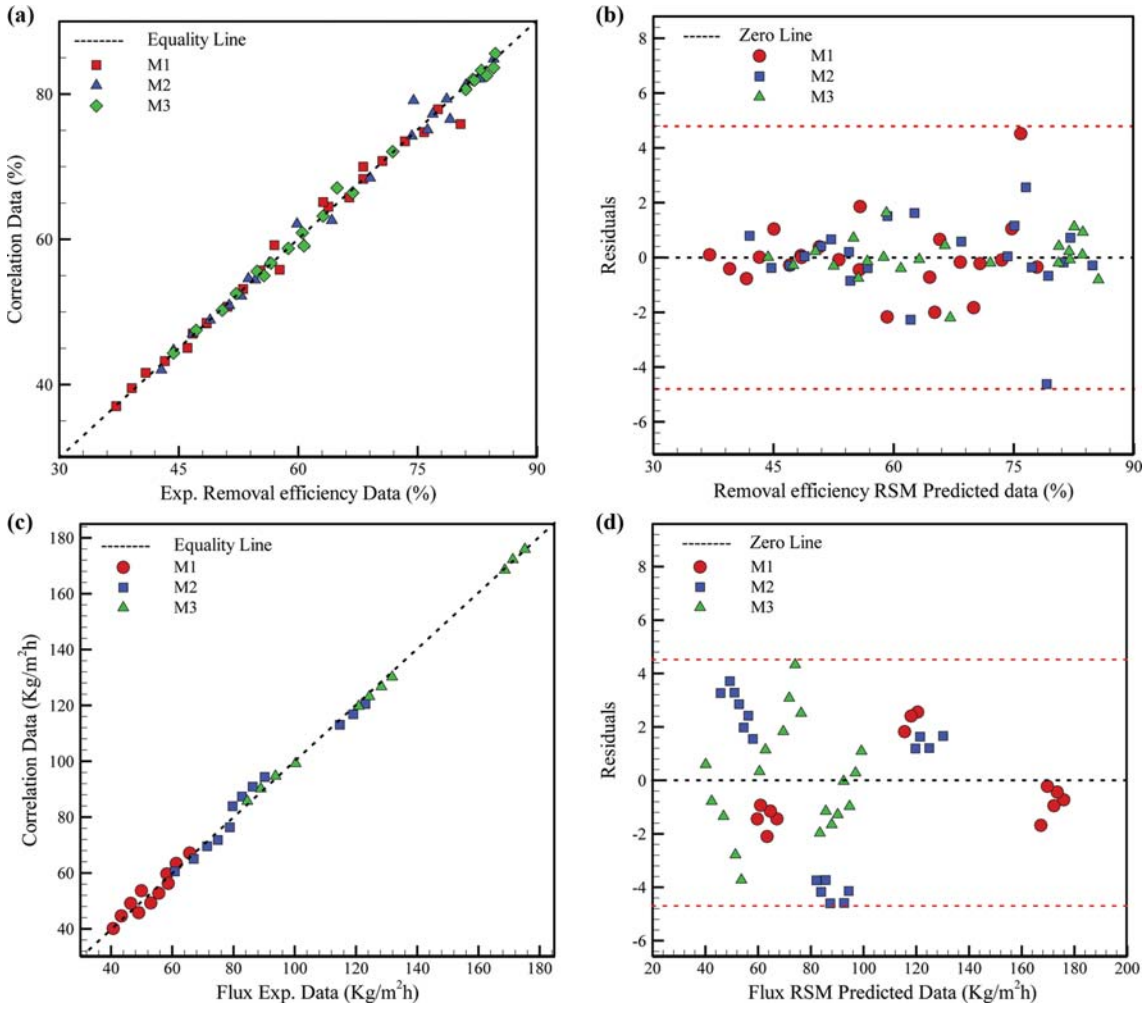

Fig. 1. The conformity and residual diagram of the proposed relationship with the experimental data: (a, b) Removal efficiency (c, d) flux.

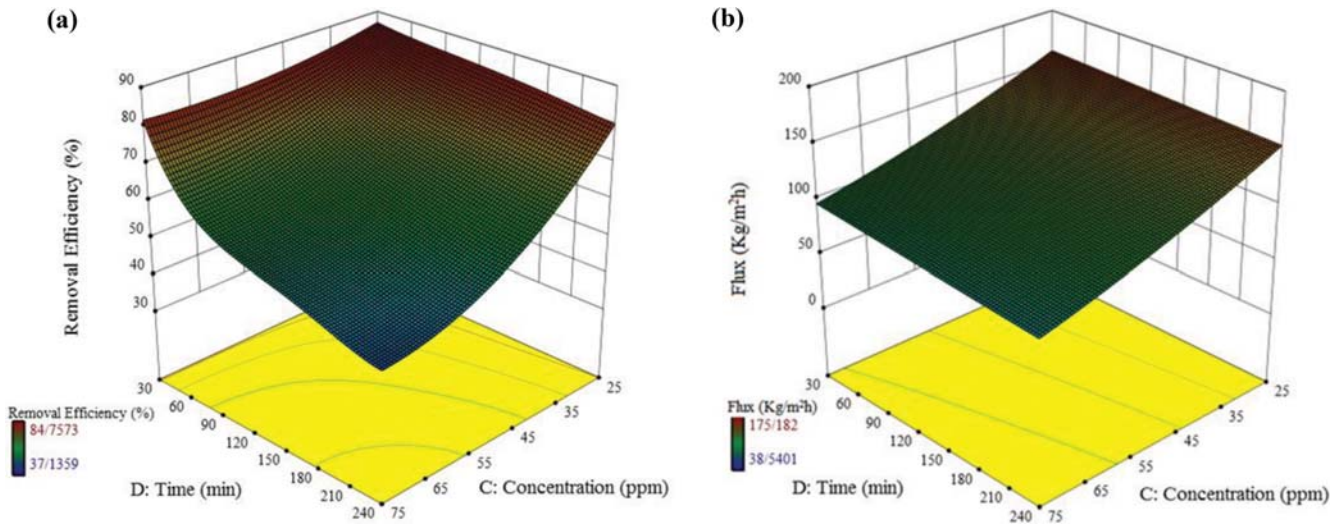

Fig. 2. 3D diagram for (a) removal efficiency (b) flux.

network are also shown in Table 4. According to the statistical analysis of the outputs of eight designed neural network structures the values of R=0.9993, R^2=0.9986, MSE=0.402 (mean square error) and MAE=0.409 (mean absolute error) for the best structure were

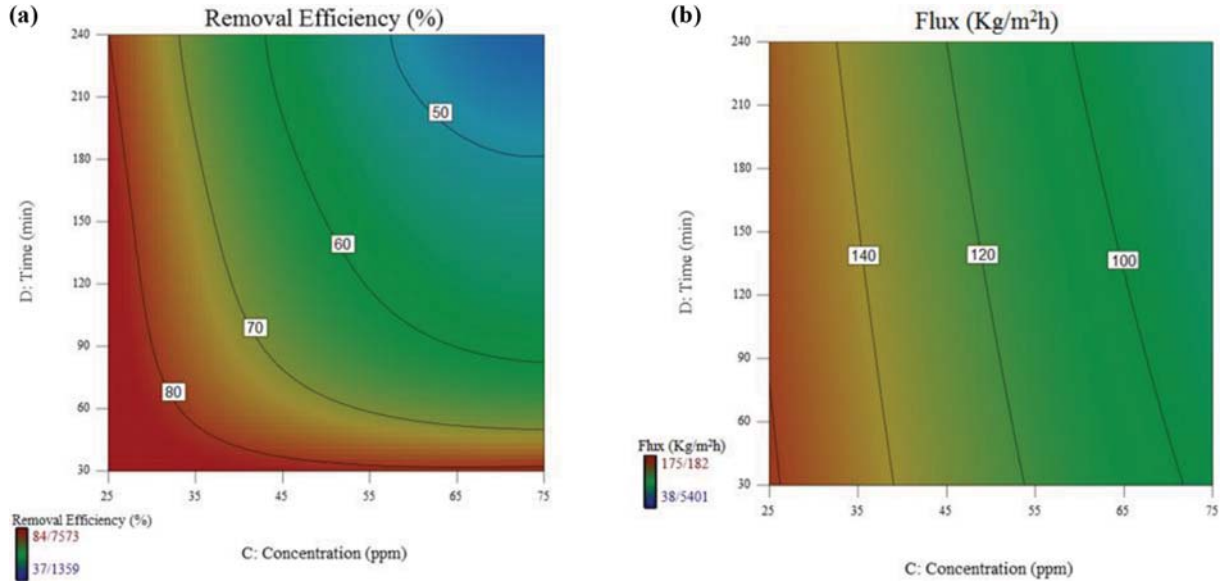

Fig. 3. Contour diagram for (a) removal efficiency (b) flux.

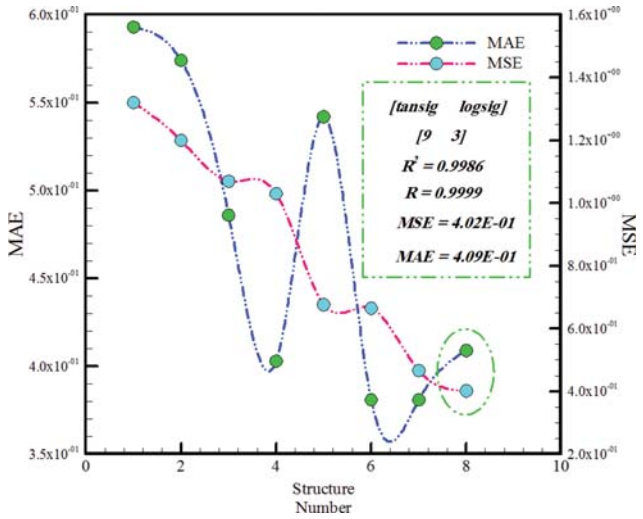

Fig. 4. MAE-MSE of MLP modeling.

obtained. Based on these values, it can be concluded that the obtained MLP model predicted the removal efficiency and permeation flux behavior successfully.

Fig. 5 illustrates the best MLP structure for predicting removal efficiency and permeate flux behavior of lead ion in aqueous solution a mixed matrix membrane [43]. As can be seen, the structure contains two hidden layers with nine (tansig transfer function) and three (logsig transfer function) neurons, respectively.

Fig. 6 shows the output charts of the MLP models versus the actual data for the parameters (a) removal efficiency and (b) flux of Pb^{2+} in solution. Due to the closeness of the points (neural network output) to the diagonal line and the low error, the precision of the obtained MLP modeling is acceptable to predict the removal efficiency and flux of lead ion in aqueous solution.

Fig. 7 shows the output error of the MLP model and the actual values for (a) removal efficiency, and (b) flux of Pb^{2+}. Given the proximity of the points to the zero lines, the proposed MLP model has good accuracy for predicting the models. As shown in Fig. 7, the maximum error for the removal efficiency model is lower than the flux model. However, many numbers of the points in the flux model are near zero lines.

3. Comparing between MLP and RSM Modeling

Fig. 8 illustrates a comparison of the compliance of MLP-ANN and RSM modeling with empirical data. For the removal efficiency and flux, both modeling methods had proper compliance with the

Table 4. ANN structures and accuracy for removal efficiency and flux modeling

Row	Structure	Transfer function	R^2	R	MAE	MSE
1	[2 8]	[tansig logsig]	0.9879	0.9942	5.93E-01	1.32E+00
2	[3 6]	[tansig tansig]	0.9894	0.9947	5.74E-01	1.20E+00
3	[3 9]	[tansig tansig]	0.9903	0.9952	4.86E-01	1.07E+00
4	[3 10]	[tansig logsig]	0.9905	0.9952	4.03E-01	1.03E+00
5	[4 5]	[logsig tansig]	0.9946	0.9973	5.42E-01	6.77E-01
6	[5 8]	[tansig logsig]	0.9945	0.9973	3.81E-01	6.65E-01
7	[8 4]	[logsig logsig]	0.9981	0.9991	3.81E-01	4.67E-01
8	**[9 3]**	**[tansig logsig]**	**0.9986**	**0.9993**	**4.09E-01**	**4.02E-01**

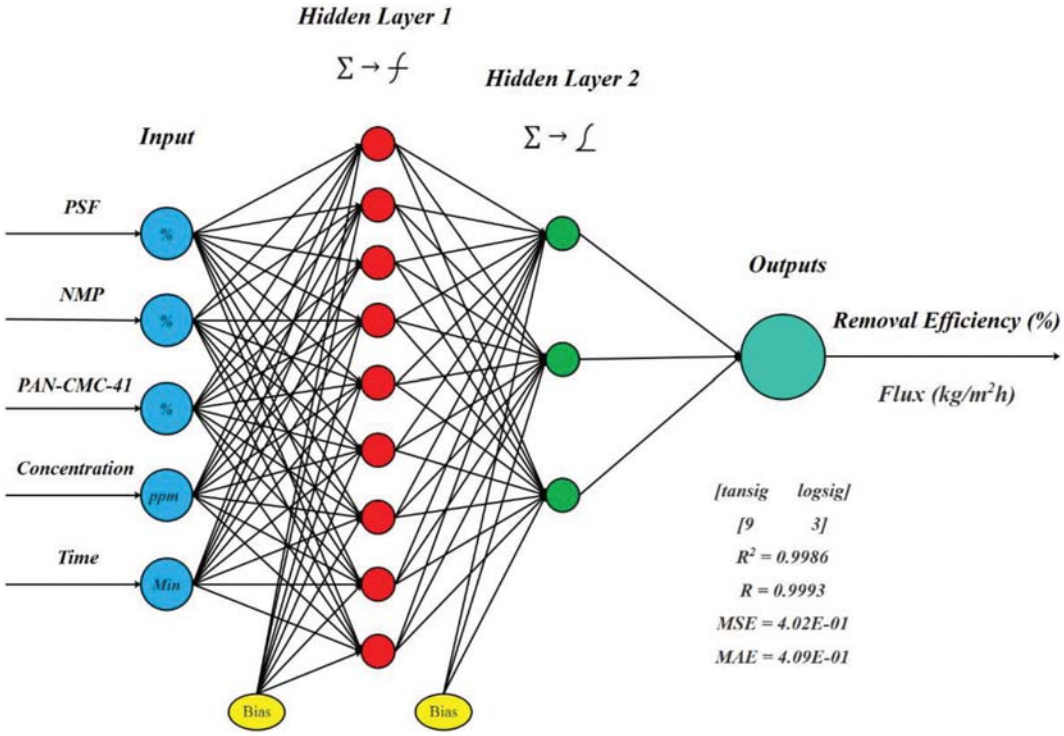

Fig. 5. Neural network structure of removal efficiency and flux modeling.

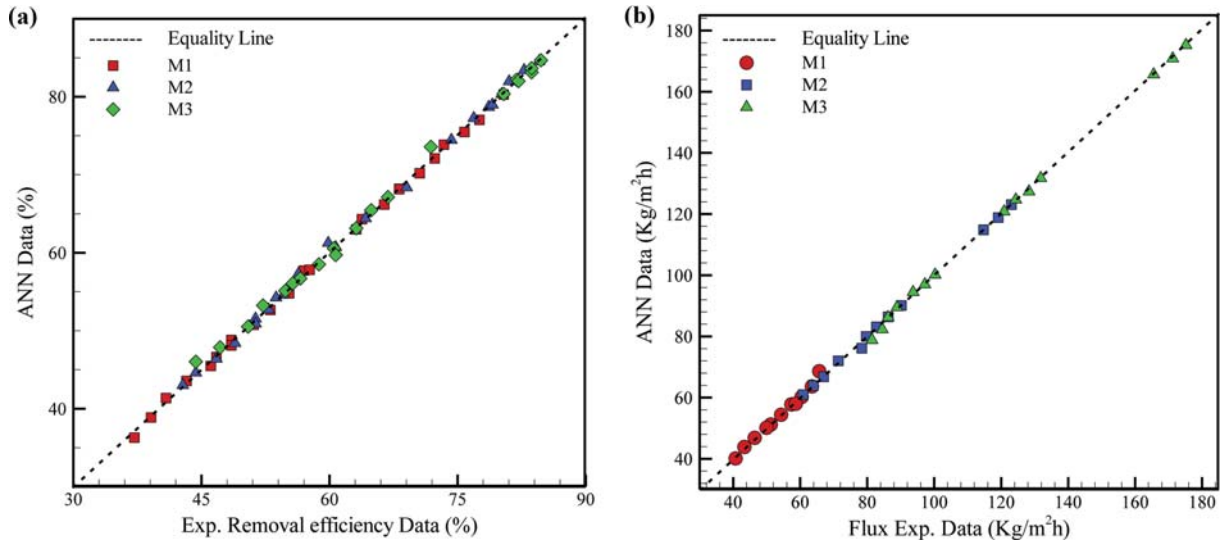

Fig. 6. Neural network matching diagram with experimental data: (a) Removal efficiency (b) flux.

observed data. However, the MLP-ANN model is more accurate than the RSM model in predicting experimental data. It can be proven by analyzing the performance data of the RSM and MLP modeling, like the R^2 value of the models. As can be seen from the R^2 value, MLP-ANN modeling has shown high accuracy in predicting the removal efficiency and flux behavior of Pb^{2+} aqueous solution in a nanofiltration process.

4. Optimization with RSM

The removal efficiency was optimized through the response surface methodology based on the experimental results of Toosi et al. [43] research. Various modes of optimization of the removal efficiency of a lead ion based on different components of the mixed matrix membrane, filtration time, and concentration of Pb^{2+} in aqueous solutions are listed in Table 5.

The best optimum state (the maximum value of removal efficiency) 3D and contour graphs are illustrated in Fig. 9. The optimum mode selected for membrane composition of PSF=10.04%, NMP=88.98%, and PAN-CMC-41=0.98% (wt%), with 53.17 ppm as lead ion concentration in solution and 30.31 min for filtration time was achieved the maximum value of removal efficiency equal 90.68%.

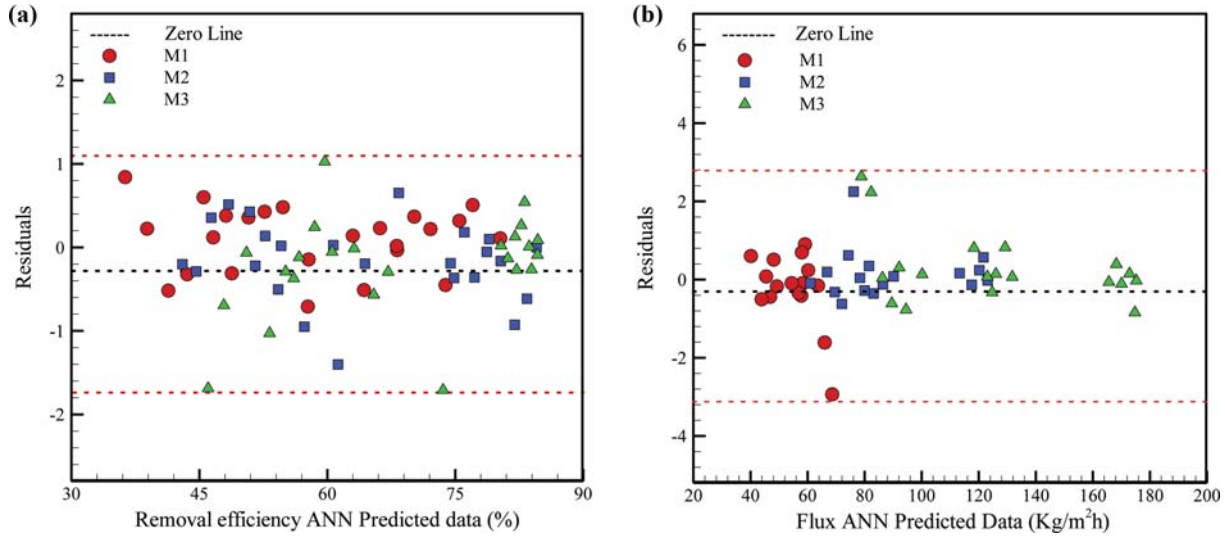

Fig. 7. Residual neural network output diagram with experimental data: (a) Removal efficiency (b) flux.

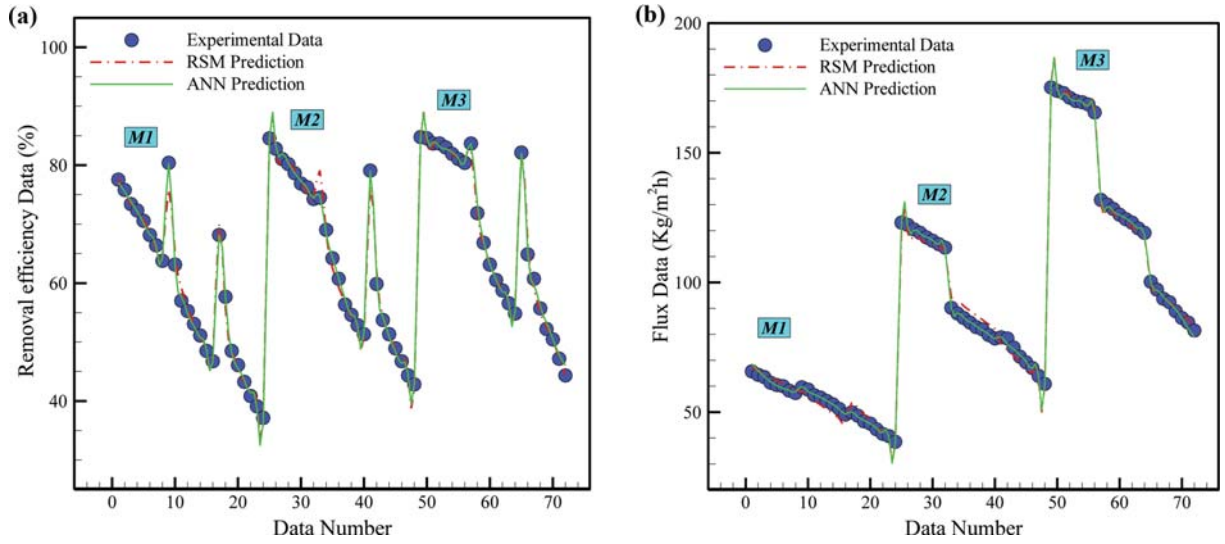

Fig. 8. Comparing between MLP-ANN and RSM modelling predication (a) removal efficiency (b) flux.

Table 5. Suggested modes of RSM optimization

Number	PSF	NMP	PAN-CMC-41	Concentration	Time	Removal efficiency	Permeate flux
1	**10.04**	**88.98**	**0.98**	**53.17**	**30.31**	**90.68**	**220.7**
2	11.37	87.75	0.88	25.34	31.6	90.3	172.38
3	11.68	87.78	0.54	25.08	30.52	90.21	176.87
4	11.44	87.95	0.61	26.42	31.22	90.08	171.54
5	11.25	87.27	1.48	25	30.22	90	170.65

CONCLUSION

Modeling of removal efficiency and permeate flux behavior for lead ion in aqueous solution using mixed matrix membranes was done successfully. Also, the removal efficiency was optimized to obtain the optimum mode of operating condition. The RSM and MLP-ANN modeling were investigated based on experimental results. Results were achieved as below:

- The RSM model has a regression coefficient R^2=0.99. The F-value for the removal efficiency and permeate flux behavior model was achieved 394.79 and 1,888.85, respectively.
- The highest amount of removal efficiency was obtained at the lowest filtration time and concentration of the lead ion. In contrast, a similar trend was obtained for the flux of lead ion.

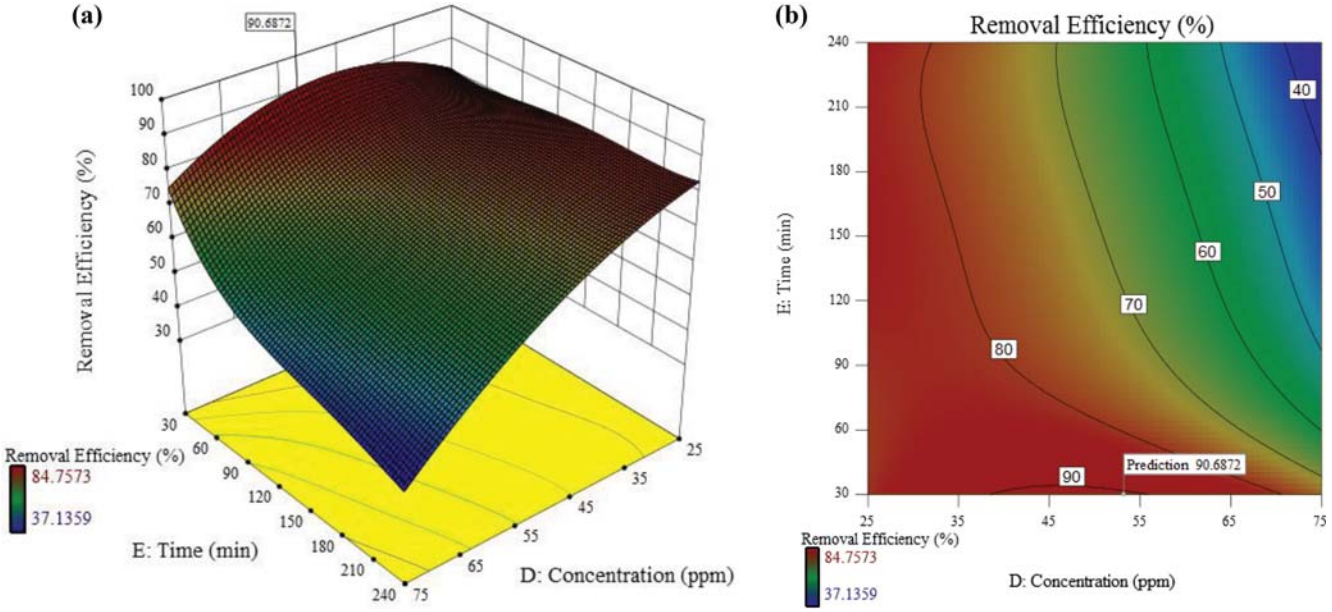

Fig. 9. RSM optimization graphs for removal efficiency (a) 3D (b) contour.

- The filtration time and concentration of Pb^{2+} both are directly related to the removal efficiency. However, the flux model, the effect of concentration, is more significant than the filtration time.
- The best MLP structure for predicting removal efficiency and permeate flux of lead ion in aqueous solution was obtained, which has two hidden layers with nine (tansig transfer function) and three (logsig transfer function) neurons.
- The values of R=0.9993, R^2=0.9986, MSE=0.402 and MAE=0.409 for the best structure were obtained.
- The optimum mode selected for membrane composition of PSF=10.04%, NMP=88.98%, and PAN-CMC-41=0.98% (wt%), with 53.17 ppm as the lead ion concentration in solution and 30.31 minutes for filtration time was achieved the maximum value of removal efficiency equal 90.68%.

ABBREVIATION CONTENT

ANN : artificial neural network
ANOVA : analysis of variance
df : degrees of freedom
DOE : design of experiments
logsig : log sigmoid transfer function
MAE : mean absolute error
MLP : multilayer perceptron
MOD : margin of deviation
MSE : mean square error
tansig : hyperbolic tangent sigmoid transfer function
R^2 : regression coefficient
RSM : response surface methodology
RMSE : root mean square error

Nomenclature

PSF : polysulfone
T : temperature [°C]
PAN : polyaniline
Pb^{2+} : lead ion
UF : ultra filtration
NF : nano filtration
RO : reverse osmosis
RE : removal efficiency

REFERENCES

1. M. Ikram, P. Zhou, S. Shah and G. Liu, *J. Clean. Prod.*, **226**, 628 (2019).
2. R. Tu, W. Jin, S.-F. Han, B. Ding, S.-h. Gao, X. Zhou, S.-f. Li, X. Feng, Q. Wang and Q. Yang, *Korean J. Chem. Eng.*, **37**, 827 (2020).
3. C. Zhang, G. Zeng, D. Huang, C. Lai, M. Chen, M. Cheng, W. Tang, L. Tang, H. Dong and B. Huang, *Chem. Eng. J.*, **373**, 902 (2019).
4. M. Deng, X. Yang, X. Dai, Q. Zhang, A. Malik and A. Sadeghpour, *Ecological Indicators*, **112**, 106166 (2020).
5. Z. Yin, L. Zhu, S. Li, T. Hu, R. Chu, F. Mo, D. Hu, C. Liu and B. Li, *Bioresour. Technol.*, **301**, 122804 (2020).
6. K. H. Vardhan, P. S. Kumar and R. C. Panda, *J. Mol.*, **290**, 111197 (2019).
7. J. Gao, K. Y. Wang and T.-S. Chung, *J. Membr. Sci.*, **603**, 118022 (2020).
8. N. G. Doménech, F. Purcell-Milton and Y. K. Gun'ko, *Mater. Today Commun.*, **23**, 100888 (2020).
9. C. Y. Foong, M. D. H. Wirzal and M. A. Bustam, *J. Mol.*, **297**, 111793 (2020).
10. N. Abdullah, R. Gohari, N. Yusof, A. Ismail, J. Juhana, W. Lau and T. Matsuura, *Chem. Eng. J.*, **289**, 28 (2016).
11. S.-Y. Tang and Y.-R. Qiu, *Korean J. Chem. Eng.*, **36**, 1321 (2019).
12. S. M. Hosseini, F. Karami, S. K. Farahani, S. Bandehali, J. Shen, E. Bagheripour and A. Seidypoor, *Korean J. Chem. Eng.*, **37**, 866 (2020).

13. V. Goel and U. K. Mandal, *Korean J. Chem. Eng.*, **36**, 573 (2019).
14. N. Nabian, A. A. Ghoreyshi, A. Rahimpour and M. Shakeri, *Korean J. Chem. Eng.*, **32**, 2204 (2015).
15. Z. Arif, N. K. Sethy, L. Kumari, P. K. Mishra and B. Verma, *Korean J. Chem. Eng.*, **36**, 1148 (2019).
16. N. Yousefi, R. Nabizadeh, S. Nasseri, M. Khoobi, S. Nazmara and A. H. Mahvi, *Korean J. Chem. Eng.*, **34**, 2342 (2017).
17. A. R. Alawady, A. A. Alshahrani, T. A. Aouak and N. M. Alandis, *Chem. Eng. J.*, **388**, 124267 (2020).
18. A. Modi and J. Bellare, *J. Water Process Eng.*, **33**, 101113 (2020).
19. L. Zhu, M. Wu, B. Van der Bruggen, L. Lei and L. Zhu, *Sep. Purif.*, **242**, 116770 (2020).
20. R. Kumar, A. M. Isloor and A. Ismail, *Desalination*, **350**, 102 (2014).
21. M. H. Esfe, M. K. Amiri and M. Bahiraei, *J. Taiwan Inst. Chem. E*, **103**, 7 (2019).
22. C.-C. Pădureţu, R. Isopescu, I. Rau, V. Schroder and M. R. Apetroaei, *Korean J. Chem. Eng.*, **36**, 1890 (2019).
23. B. Kim, Y. Choi, J. Choi, Y. Shin and S. Lee, *Korean J. Chem. Eng.,* **37**, 1 (2020).
24. M. H. Esfe, M. H. Kamyab, M. Afrand and M. K. Amiri, *Pkysica A*, **510**, 610 (2018).
25. S. Yildiz, *Korean J. Chem. Eng.*, **34**, 2423 (2017).
26. M. H. Esfe, H. Rostamian, M. Rejvani and M. R. S. Emami, *Physica E Low Dimens. Syst. Nanostruct.*, **102**, 160 (2018).
27. A. A. Prabhu, B. Mandal and V. V. Dasu, *Korean J. Chem. Eng.*, **34**, 1109 (2017).
28. S. P. G. Zaferani, M. R. S. Emami, M. K. Amiri and E. Binaeian, *Int. J. Biol. Macromol.*, **139**, 307 (2019).
29. M. Pazouki, M. Zabihi, J. Shayegan and M. H. Fatehi, *Korean J. Chem. Eng.*, **35**, 671 (2018).
30. F. Hosseini and M. Rahimi, *Korean J. Chem. Eng.*, **37**, 411 (2020).
31. H. Karimnezhad, A. H. Navarchian, T. T. Gheinani and S. Zinadini, *Chem. Eng. Res. Des.*, **153**, 187 (2020).
32. M. M. Baneshi, A. M. Ghaedi, A. Vafaei, D. Emadzadeh, W. J. Lau, H. Marioryad and A. Jamshidi, *Environ. Res.*, **183**, 109278 (2019).
33. Y. Chen, L. Shen, R. Li, X. Xu, H. Hong, H. Lin and J. Chen, *J. Colloid Interface Sci.*, **565**, 1 (2020).
34. J. Farahbakhsh, M. Delnavaz and V. Vatanpour, *J. Membr. Sci.*, **581**, 123 (2019).
35. K. Ho, *Process Saf. Environ.*, **126**, 297 (2019).
36. F. Schmitt, R. Banu, I.-T. Yeom and K.-U. Do, *Biochem. Eng. J.*, **133**, 47 (2018).
37. Z. Seifollahi and A. Rahbar-Kelishami, *J. Mol.*, **231**, 1 (2017).
38. M.-J. Corbatón-Báguena, M.-C. Vincent-Vela, J.-M. Gozálvez-Zafrilla, S. Álvarez-Blanco, J. Lora-García and D. Catalán-Martínez, *Sep. Purif.*, **170**, 434 (2016).
39. A. Tiwari, D. Pal and O. Sahu, *Res-Eff Tech.*, **3**, 37 (2017).
40. A. Alver and Z. Kazan, *Sep. Purif.*, **230**, 115868 (2020).
41. P. Choudhury, P. Mondal, S. Majumdar, S. Saha and G. C. Sahoo, *J. Clean. Prod.*, **203**, 511 (2018).
42. L. Y. Jun, R. R. Karri, L. S. Yon, N. Mubarak, C. H. Bing, K. Mohammad, P. Jagadish and E. Abdullah, *Environ. Res.*, **183**, 109158 (2020).
43. M. R. Toosi, M. R. S. Emami and S. Hajian, *Environ. Sci. Pollut.*, **25**, 20217 (2018).
44. M. Kalaiyarasi, P. Ahmad and P. Vijayaraghavan, *J. King Saud Univ. Sci.*, **32**, 2134 (2020).
45. A. Poorarbabi, M. Ghasemi and M. A. Moghaddam, *Ain Shams Eng. J.*, In press (2020). https://doi.org/10.1016/j.asej.2020.02.009.
46. H. Zhang, J. P. Choi, S. K. Moon and T. H. Ngo, *Addit. Manuf.*, **33**, 101096 (2020).
47. N. Ratanasumarn and P. Chitprasert, *Int. J. Biol. Macromol.*, **153**, 138 (2020).
48. M. Hosseinpour, M. Soltani, A. Noofeli and J. Nathwani, *Fuel*, **271**, 117618 (2020).
49. M. Fayed, M. Elhadary, H. A. Abderrahmane and B. N. Zakher, *Alex. Eng. J.*, **58**, 1367 (2020).
50. H. H. Alkinani, A. T. T. Al-Hameedi, S. Dunn-Norman and D. Lian, *Egypt. J. Pet.*, **173**, 1097 (2019).
51. M. Juez-Gil, I. N. Erdakov, A. Bustillo and D. Y. Pimenov, *J. Adv. Res.*, **18**, 173 (2019).
52. Z. Alameer, M. A. Elaziz, A. A. Ewees, H. Ye and Z. Jianhua, *Resources Policy*, **61**, 250 (2019).